

Differing roles for members of the phospholipase A₂ superfamily in experimental autoimmune encephalomyelitis

Athena Kalyvas,¹ Constantinos Baskakis,² Victoria Magrioti,² Violetta Constantinou-Kokotou,³ Daren Stephens,⁴ Rubèn López-Vales,¹ Jian-Qiang Lu,^{5,6} V. Wee Yong,^{5,6} Edward A. Dennis,⁴ George Kokotos² and Samuel David¹

1 Center for Research in Neuroscience, Research Institute of the McGill University Health Center, Montreal, Quebec, Canada H3G 1A4

2 Department of Chemistry, University of Athens, Greece

3 Chemical Laboratories, Agricultural University of Athens, Greece

4 Department of Chemistry & Biochemistry, School of Medicine, University of California, San Diego, USA

5 Department of Clinical Neurosciences, University of Calgary, Calgary, Alberta, Canada

6 Department of Oncology, University of Calgary, Calgary, Alberta, Canada

Correspondence to: Dr Samuel David,
Center for Research in Neuroscience,
McGill University Health Center Research Institute,
Livingston Hall, Room L7-210, 1650 Cedar Ave.,
Montreal, Quebec,
Canada H3G 1A4
E-mail: sam.david@mcgill.ca

The phospholipase A₂ (PLA₂) superfamily hydrolyzes phospholipids to release free fatty acids and lysophospholipids, some of which can mediate inflammation and demyelination, hallmarks of the CNS autoimmune disease multiple sclerosis. The expression of two of the intracellular PLA₂s (cPLA₂ GIVA and iPLA₂ GVIA) and two of the secreted PLA₂s (sPLA₂ GIIA and sPLA₂ GV) are increased in different stages of experimental autoimmune encephalomyelitis (EAE), an animal model of multiple sclerosis. We show using small molecule inhibitors, that cPLA₂ GIVA plays a role in the onset, and iPLA₂ GVIA in the onset and progression of EAE. We also show a potential role for sPLA₂ in the later remission phase. These studies demonstrate that selective inhibition of iPLA₂ can ameliorate disease progression when treatment is started before or after the onset of symptoms. The effects of these inhibitors on lesion burden, chemokine and cytokine expression as well as on the lipid profile provide insights into their potential modes of action. iPLA₂ is also expressed by macrophages and other immune cells in multiple sclerosis lesions. Our results therefore suggest that iPLA₂ might be an excellent target to block for the treatment of CNS autoimmune diseases, such as multiple sclerosis.

Keywords: EAE; multiple sclerosis; Phospholipase A₂; fatty acids; chemokines; cytokines

Abbreviations: DPA = docosapentanoic acid; EAE = Experimental autoimmune encephalomyelitis; FACS = Fluorescence activated cell sorting; PLA₂ = phospholipase A₂

Introduction

Multiple sclerosis is a multi-focal autoimmune demyelinating disease of the CNS (Compston and Coles, 2002; Steinman *et al.*, 2002). The clinical symptoms include paralysis, sensory loss and autonomic dysfunction, as the focal lesions can occur in widespread regions of the CNS (Noseworthy *et al.*, 2000). Experimental autoimmune encephalomyelitis (EAE) is a widely used rodent model (Gold *et al.*, 2006; Steinman and Zamvil, 2006; Baxter, 2007), which has provided important insights into some of the mechanisms underlying CNS autoimmune disease. Although T cells mediate the disease, macrophages and CNS glia contribute importantly to the CNS pathology. The exact mechanisms underlying the formation of these lesions in the CNS are still not fully understood.

PLA₂ consists of a large superfamily that includes secreted (sPLA₂) and intracellular cytosolic PLA₂s. They hydrolyze ester bonds at the *sn*-2 position of membrane phospholipids to generate free fatty acids and lysophospholipids (Kudo and Murakami, 2002; Schaloske and Dennis, 2006). Arachidonic acid released by PLA₂, via the cyclooxygenase (COX) and lipoxygenase pathways, can give rise to eicosanoids such as prostaglandins (PG) and leukotrienes (Calder, 2003; Rocha *et al.*, 2003) that contribute to various aspects of inflammation. In addition, one of the other products of PLA₂, lysophosphatidylcholine, can also contribute to these inflammatory changes as it can induce the expression of chemokines and cytokines (Ousman and David, 2001), and is also a potent demyelinating agent (Ousman and David, 2000). Therefore, PLA₂ could set off a robust inflammatory and demyelinating response in the CNS in multiple sclerosis and EAE via multiple pathways.

The C57BL/6 mouse strain has a naturally occurring null mutation of a major form of sPLA₂ [group IIA (GIIA)] (Kennedy *et al.*, 1995). Using this mouse strain, we showed previously that arachidonyl trifluoromethyl ketone (AACOCF₃), a non-selective inhibitor that blocks various forms of the intracellular cytosolic PLA₂s, markedly reduces the onset and progression of the disease (Kalyvas and David, 2004). Additionally, cPLA₂ GIVA knockout mice on the C57BL/6 background are resistant to EAE (Marusic *et al.*, 2005).

We now present evidence that of the 14 members of the PLA₂ superfamily that are expressed in SJL/J mice, four change their expression in EAE. We have characterized the expression of these four PLA₂s in different stages of EAE, and using selective inhibitors show that cPLA₂ and iPLA₂ appear to play different roles in the onset and progression of the disease. Additional work on chemokine and cytokine expression and lipid profiling revealed some of the potential mechanisms underlying these effects.

Materials and Methods

Generation of EAE

EAE was induced in female SJL/J mice by subcutaneous injections of 100 µg of proteolipid protein (Sheldon Biotechnology Centre, Montreal, Canada) in Complete Freund's Adjuvant (CFA) [Incomplete Freund's adjuvant containing 4 mg/ml of heat inactivated

Mycobacterium tuberculosis (Fisher Scientific, Nepean, Canada)]. Mice were boosted on Day 7 with 50 µg of proteolipid protein in CFA containing 2 mg/ml of heat inactivated *M. tuberculosis*. The mice were monitored daily for clinical symptoms of EAE using the following scale: grade 0 = normal (no clinical signs), grade 0.5 = tail weakness (partial flaccid tail), grade 1 = tail paralysis (complete flaccid tail), grade 2 = mild hindlimb weakness (fast righting reflex), grade 3 = severe hindlimb weakness (slow righting reflex), grade 4 = hindlimb paralysis, grade 5 = hindlimb paralysis and forelimb weakness or moribund. The person doing the clinical monitoring was blind to the experimental groups.

Double immunofluorescence

Mice at different clinical stages [onset (11–12 days), peak (18 days), remission (20–25 days)] were deeply anesthetized and intracardially perfused with 0.1 M phosphate buffer followed by perfusion with 4% paraformaldehyde in 0.1 M phosphate buffer. Cryostat sections (12 µm) were blocked in 0.1% Triton-X 100 and 10% normal goat serum and incubated overnight with polyclonal anti-cPLA₂ GIVA (Santa Cruz Biotechnology, 1:75), anti-iPLA₂ GVIA, anti-sPLA₂ IIA or anti sPLA₂V (Cayman Chemicals, 1:500, 1:100, 1:100, respectively) combined with monoclonal antibodies specific for astrocytes (mouse anti-GFAP, Sigma, 1:1000) or oligodendrocytes (mouse anti-APC, Calbiochem, 1:30). This was followed by incubation with a biotinylated goat anti-rabbit secondary antibody (Jackson ImmunoResearch Laboratories, 1:400) combined with a goat anti-mouse rhodamine-conjugated secondary antibody (Jackson ImmunoResearch Laboratories, 1:200). After washing, the sections were incubated with fluorescein-conjugated streptavidin (Molecular Probes, 1:400).

Histochemistry and immunohistochemistry of postmortem multiple sclerosis tissue

The tissue analysed in this study was from archival paraffin-embedded blocks and its use for research was approved by the University of Calgary Research Ethics Board. Tissue was obtained at autopsy from three patients with multiple sclerosis (25-year-old male, 34-year-old female and 38-year-old female; postmortem delay of <24 h). The diagnosis of multiple sclerosis was confirmed by a neuropathologist. Coexisting neuropathology was excluded. The tissue blocks containing multiple sclerosis lesions were sampled from various CNS regions particularly the spinal cord. The multiple sclerosis lesions were classified into active, chronic active and chronic inactive lesions, based on the Bo/Trapp staging system (Trapp *et al.*, 1998; van der Valk and De Groot, 2000). All cases had active lesions and/or chronic active lesions (data not shown). Active lesions were actively demyelinating and acutely inflammatory throughout the lesion, with heavy infiltration of CD3⁺ T cells and CD68⁺ macrophages, as well as damaged axons immunoreactive for amyloid precursor protein; chronic active lesions were hypocellular in the cores, but hypercellular along the edges that contained focal demyelinating and inflammatory activity.

Tissue sections (6 µm) were deparaffinized, rehydrated and antigen retrieval performed in sodium citrate (pH 6.0) for 20 min at 95°C. Sections were washed with PBS, placed in 2% H₂O₂ for 10 min at room temperature and blocked in 0.1% Triton-X containing 2% normal donkey serum and 1% ovalbumin. For immunofluorescence, sections were incubated overnight with polyclonal iPLA₂ GVIA and a rat monoclonal anti-Mac-2 (1:2, hybridoma supernatant) to identify

activated macrophages. Sections were washed and visualized by incubation with Alexa 488-conjugated donkey anti-rabbit (1:400, Molecular Probes), and Alexa544-conjugated donkey anti-rat (1:400, Molecular Probes). Another series of sections was stained with Luxol fast blue and hematoxylin to identify the areas of demyelination.

Fluorescence activated cell sorting

Mice were anesthetized at the onset, peak and remission stages and intracardially perfused with 20 ml of PBS. Brains and spinal cords, and spleens from six mice were collected and dissociated at each stage of disease, into a single-cell suspension by passing through a 70 µm pore size cell strainer (BD Biosciences). After centrifugation with 37% Percoll (Amersham Biosciences), cells were resuspended in buffer containing mouse IgG to block non-specific antibody binding. These cells were then stained with the following antibodies: Polyclonal rabbit anti-cPLA₂, anti-iPLA₂, anti-sPLA₂IIA and anti-sPLA₂V; monoclonal, FITC-conjugated anti-CD4, anti-CD8, anti-Mac-1/CD11b and anti-CD11c, (BD Pharmingen, 1:200). Goat anti-rabbit biotin and PE-conjugated streptavidin were sequentially added thereafter. Cells were isolated using a Fluorescence activated cell sorting (FACS) Vantage cell sorter (BD Immunocytometry Systems-Lyman Duff Medical Building), and flow cytometry data were analysed using the CellQuest software. The FACS analysis of the different immune cell types was repeated four times.

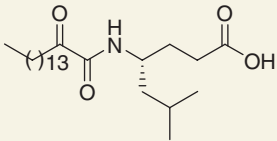
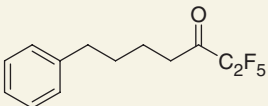
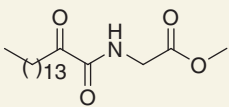
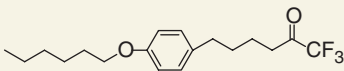
Treatment of EAE-induced mice

Two classes of PLA₂ inhibitors were used: the 2-oxoamides (AX059 and AX115) and fluoroketones (FKGK11 and FKGK2). The 2-oxoamide inhibitors have been extensively characterized (Kokotos *et al.*, 2004; Stephens *et al.*, 2006; Six *et al.*, 2007). Some of these such as AX059

is selective and potent inhibitors of cPLA₂ GIVA (Table 1), and have been used in other *in vivo* models (Kokotos *et al.*, 2002, 2004; Stephens *et al.*, 2006; Yaksh *et al.*, 2006; Six *et al.*, 2007). AX059 shows >95% inhibition of cPLA₂ at 0.091 mole fraction, while showing 0% inhibition of iPLA₂ and sPLA₂ (Table 1). Its X₁(50) value, which is the mole fraction of the inhibitor in the total substrate interface required to inhibit the enzyme by 50%, is 0.008 ± 0.002, indicating high potency. One of the fluoroketones (FKGK11) is a selective and potent inhibitor of iPLA₂ (Table 1) and has been used *in vivo* (Lopez-Vales *et al.*, 2008). Details of the synthesis and further data on the inhibition by these novel fluoroketone compounds are described elsewhere (Baskakis *et al.*, 2008). FKGK11 is highly selective for iPLA₂ GVIA, showing >95% inhibition of iPLA₂ at 0.091 mole fraction as compared to inhibiting only 17% of cPLA₂ and 29% of sPLA₂. At the high concentration of substrate used for these assays, values of 25% or below are not considered significant. Its X₁(50) value (0.0073 ± 0.0007) also indicates that it is a potent inhibitor of iPLA₂. In addition, two pan-PLA₂ inhibitors were used, one of which strongly inhibits all three PLA₂s (the fluoroketone, FKGK2); the other is a weak pan-inhibitor (the 2-oxoamide, AX115). However, the free acid generated by the hydrolysis of AX115 inhibits sPLA₂ (IC₅₀ = 4.2 µm; M. Gelb and G. Kokotos, unpublished results). Therefore, AX115 could potentially block sPLA₂ more than cPLA₂ and iPLA₂.

EAE-induced mice were randomly assigned to the treatment and control groups. For the groups that received treatment before the onset of clinical symptoms, treatment was started on Day 5 after immunization and given daily for 3 weeks. Daily injections of the compounds AX059, AX115, FKGK11 and FKGK2 were given on a 3-day cycle consisting of one intravenous injection (100 µl) followed by two intraperitoneal injections (200 µl) of a 2 mM solution. Mice in the control group were treated with the vehicle used to suspend the inhibitors, i.e. PBS containing 5% Tween 80. For the groups that

Table 1 Selectivity and X₁(50) values of the PLA₂s inhibitors used

Inhibitor	Structure	Percentage inhibition and X ₁ (50) values		
		cPLA ₂	iPLA ₂	sPLA ₂
AX059 cPLA ₂ inhibitor		>95 X ₁ (50) = 0.008 ± 0.002	0	0
FKGK 11 iPLA ₂ inhibitor		17	>95 X ₁ (50) = 0.0073 ± 0.0007	29
AX115 pan inhibitor		62	45	52
FKGK2 pan PLA ₂ inhibitor		92 X ₁ (50) = 0.0098 ± 0.0006	91 X ₁ (50) = 0.0169 ± 0.0021	86

Structural features, selectivity data and X₁(50) values for the 2-oxoamide and fluoroketone compounds used to differentially block the various forms of PLA₂. The percentage inhibition shown in this Table denotes the selectivity of these compounds for the different PLA₂s tested, and the X₁(50) values denote their potency (see Materials and methods section for further details).

received delayed treatment after symptoms occurred, mice were treated with daily intraperitoneal injections of AX059, FKGG11 and FKGG2 starting from the first day of clinical symptoms [grade of 0.5, (tail weakness) starting either at Day 11 or 12]; and AX115 starting from just before the clinical peak (Day 14). All inhibitors were administered for 2 weeks.

Mouse inflammation antibody array

Spinal cords were removed from vehicle- and inhibitor-treated animals when the vehicle-treated mice reached the peak of disease (score of 4). The tissues were then homogenized in lysis buffer and centrifuged at 1000g. These protein samples were then assessed using the Raybio® inflammatory antibody array from RayBiotech Inc (Norcross, GA). Briefly, blocking buffer was added to glass-chip slides, which are coated with antibodies against chemokine, cytokine and related proteins. The slides were then incubated with the various protein samples from the treatment and control groups. After washing the glass slides, they were incubated sequentially with a biotin conjugated secondary antibody solution, horseradish peroxidase (HRP)-conjugated streptavidin, and HRP detection buffer. The signals were then visualized by chemiluminescence. Densitometric analysis was performed to detect differences between the various samples using ImageQuant 5.1 software (Molecular Dynamics). Positive control signals were used to normalize the level of expression from different glass slides being compared. Tissue from one mouse was used for each experiment, and the experiments repeated three times with samples from three different mice ($n=3$ for each group). All the detection and analysis were done blind.

Lipid profiling

Spinal cords were removed from vehicle- and inhibitor-treated animals at the peak stage of disease when the vehicle-treated mice reached the clinical score of 4, and the tissue snap frozen in liquid nitrogen. Lipid profiling was carried out by Lipomics Technology Inc. (West Sacramento, CA). The tissues were then extracted for either TrueMass® lipid profiling, or an eicosanoid inflammatory panel analysis. The lipids from the tissues were extracted in the presence of authentic internal standards as previously described (Folch *et al.*, 1957), using chloroform:methanol (2:1 v/v). Individual lipid classes within each extract were separated by liquid chromatography (Agilent Technologies model 1100 Series). Each lipid class was *trans*-esterified in 1% sulphuric acid in methanol in a sealed vial under a nitrogen atmosphere at 100°C for 45 min. The resulting fatty acid methyl esters were extracted from the mixture with hexane containing 0.05% butylated hydroxytoluene and prepared for gas chromatography by sealing the hexane extracts under nitrogen. Fatty acid methyl esters were separated and quantified by capillary gas chromatography (Agilent Technologies model 6890) equipped with a 30 m DB-88MS capillary column (Agilent Technologies) and a flame ionization detector. Lipomic Surveyor® software was used to visualize changes within the treated groups. Tissue from one mouse was used for each experiment and the experiments repeated three times with samples from three different mice ($n=3$ for each group). All the detection and analysis were done blind.

Eicosanoid analysis

Lipids extracted from tissues using solid phase extraction in the presence of a mixture of deuterium labelled surrogates. The mass of the sample and the surrogate standards were used to calculate the

quantitative amount of each analyte in the test matrix. Each sample was analysed by LC/MSMS, using Phenomenex Luna C18 reverse phase column (150 × 2.1 mm) connected to a Waters Quattro Premier triple quadrupole mass spectrometer. The analytes were ionized via negative electrospray and the mass spectrometer was operated in the tandem mass spec mode. An analytical software (MassLynx V4.0 SP4 2004, Waters Corporation) was used to identify target analytes based on the reference standard to generate a profile. Experiments were repeated with three times with samples from three different mice ($n=3$), and all the detection and analysis between treatment groups was done blind.

Statistical analyses

Data are shown as mean ± SEM. Statistical analyses of the results of the functional assessments were performed by using two-way repeated measures Friedman's ANOVA on Ranks. All other analyses were carried out using the student's *t*-test. Differences were considered significant if $P < 0.05$.

Results

PLA₂ isoforms are expressed differentially at various stages of EAE

Changes in mRNA expression

We first assessed the mRNA expression of four intracellular PLA₂s including calcium dependent [cPLA₂ (IVA, IVB)] and calcium independent [iPLA₂ (VIA, VIB)] forms, as well as 10 sPLA₂s (IIA, IIC, IID, IIE, IIF, V, VII, X, XII-1, XII-2) in the spinal cord and spleen of SJL/J mice at the onset, peak and remission stages of EAE. The mRNA expression of cPLA₂ GIVA is increased mainly at the onset of EAE in the spinal cord and spleen (Fig. 1A and B), while iPLA₂ GVIA is increased at the onset and peak stages of the disease in the spinal cord, and highest at the peak in the spleen (Fig. 1A and B; unchanged PLA₂s not shown). In contrast, sPLA₂ GIIA is increased at the peak in the spinal cord and at the peak and remission stages in the spleen, while sPLA₂ GV is increased in the peak and remission stages in the spinal cord and spleen (Fig. 1A and B). Changes in the expression of these PLA₂s in the spinal cord are likely to be due to expression in the immune cells that are recruited and/or expression in CNS glia.

Changes in protein expression in immune cells

The four PLA₂s that showed changes at the mRNA level was assessed by FACS analysis of immune cells isolated from the CNS and spleen (Fig. 2A and B; and Supplementary Fig. 1). The expression of all four PLA₂s at the onset of EAE is predominately in CD11b⁺ macrophages (Fig. 2A), followed by CD4⁺ T cells, CD8⁺ T cells and dendritic cells (Fig. 2A). At the peak stage, the proportion of T cells that express all four groups of PLA₂ is highest (Fig. 2A). In the remission stage, cPLA₂ IVA and sPLA₂ IIA are expressed mainly by macrophages. Overall, all PLA₂s are expressed at much lower levels in the spleen than in the CNS (Fig. 2B). Collectively, these data indicate that there is a marked increase in the proportion of macrophages and T cells that express the four PLA₂s after

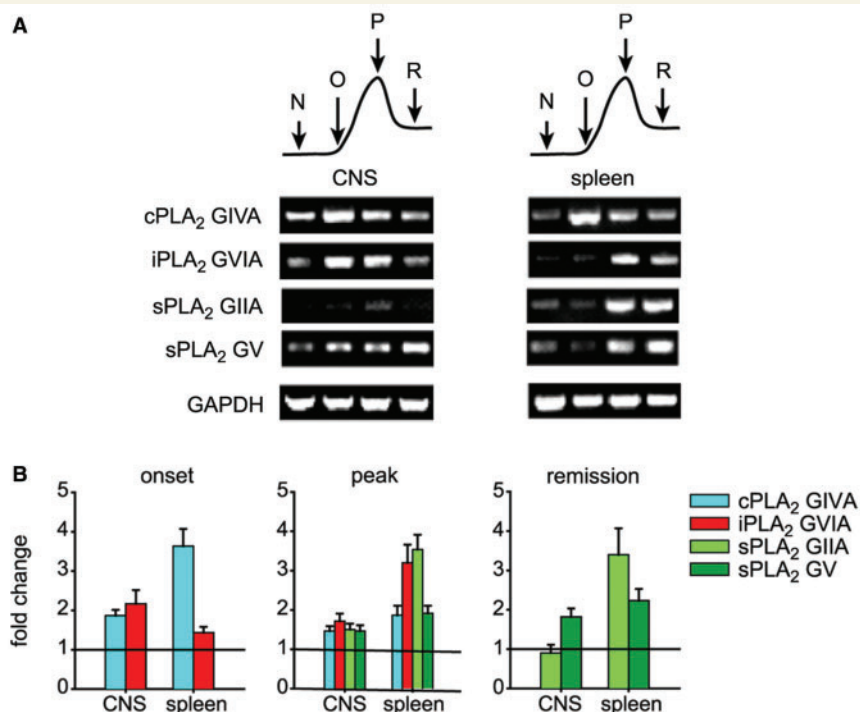


Figure 1 Expression of PLA₂s in EAE. (A) RT-PCR showing the changes in the expression of four PLA₂s in the spinal cord (CNS) and spleen in normal mice (N), and at the onset (O), peak (P) and remission (R) stages of EAE. RNA was isolated using the RiboPure™ kit (Ambion Inc, Austin, TX) and RT-PCR performed using the GeneAmp RNA PCR kit (Perkin-Elmer Life Sciences). The primers and conditions used are listed in Supplementary Table 1. (B) Quantification of the RT-PCR data showing the fold increase in mRNA expression at the onset, peak, and remission stages of EAE as compared to normal mice. Data presented as means ± SEM from three mice ($n=3$).

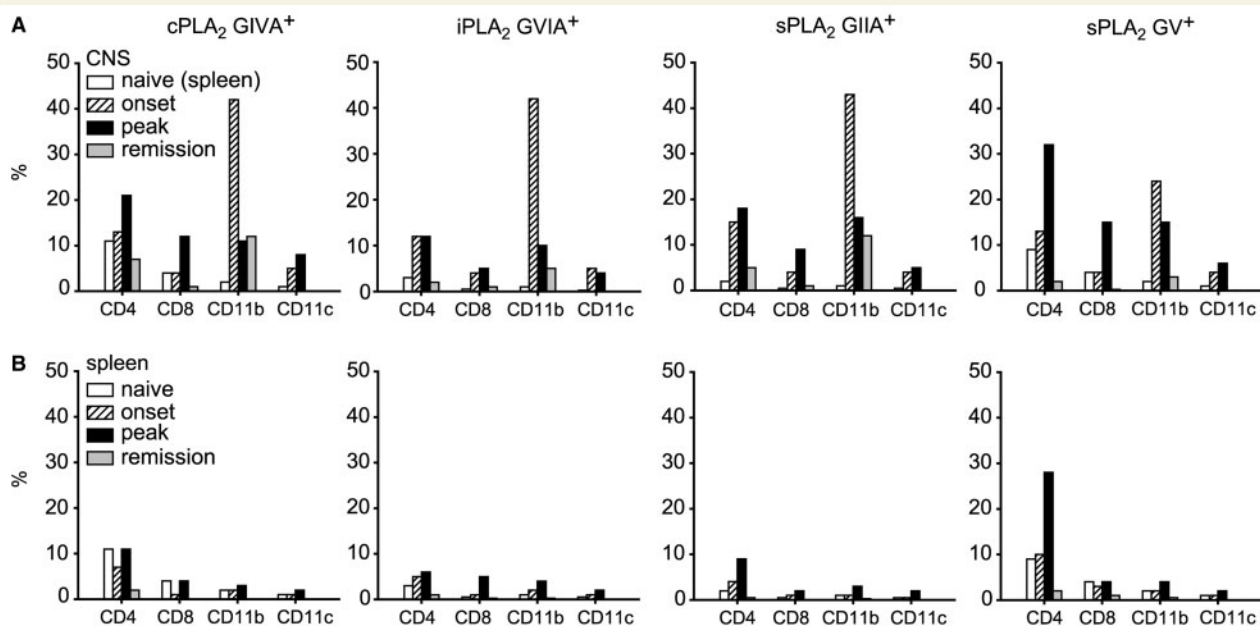


Figure 2 FACS analysis data showing the percentage of different immune cell populations that express the four PLA₂s from cells isolated from the CNS (A) and spleen (B) at the onset, peak and remission stages of EAE. Note that the numbers of positive cells is markedly higher in the CNS than in the spleen. (also see Supplementary Fig. 1).

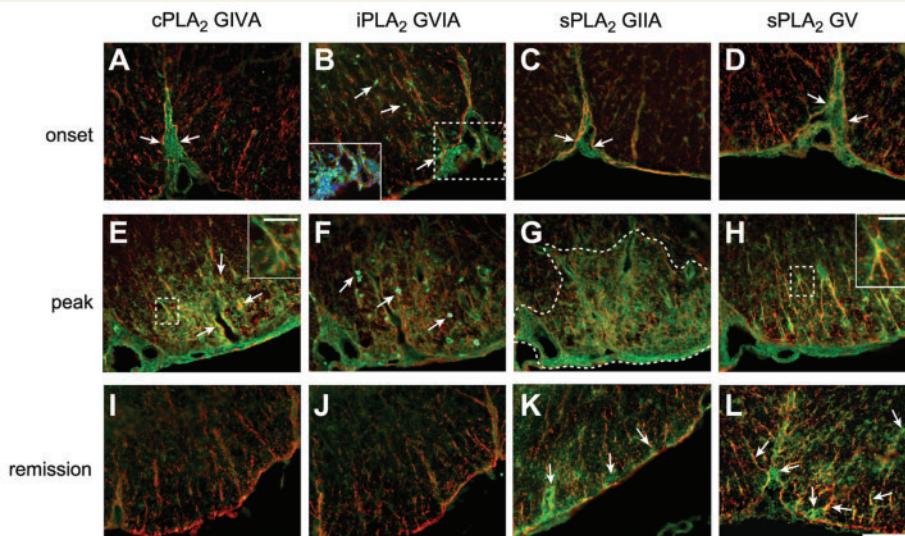


Figure 3 Micrographs showing the ventral region of the lumbar spinal cord double-labelled with anti-GFAP (red) and anti-PLA₂ (green) antibodies. The PLA₂ labelling is indicated at the top of each panel. (A–D) Note that at the onset of disease, the expression of all PLA₂s is seen in immune cell infiltrates in the submeningeal regions (arrows). The inset in panel B is a higher magnification of the area outlined in the box showing iPLA₂ labelling and nuclear labelling (DAPI), indicating the presence of immune cell infiltrates in this region. (E–H) At the peak of disease there is a marked increase in all PLA₂s. The co-localization of cPLA₂ GIVA and sPLA₂ GV in GFAP⁺ astrocytes is illustrated in the inserts which show higher magnification of the boxed areas in panels E and H. iPLA₂ GVIA labelling is very prominent in what appear to be immune cells (arrows in F), while the sPLA₂ GIIA labelling is very diffuse in the area outlined by the dashed line in panel G. sPLA₂ GV (H) also shows some diffuse labelling in addition to the labelling of astrocytes. (I–L) In the remission stage there is little if any expression of cPLA₂ GIVA (I) and iPLA₂ GVIA (J) but there is still expression of sPLA₂ GIIA and V (K and L). Scale bar = 100 µm. Scale bars in insets = 30 µm.

they enter the CNS in EAE, as compared to their initial site of activation in the spleen.

Changes in immunofluorescence staining of spinal cord tissue

In naïve mice, there is low-constitutive expression of all four PLA₂s in some astrocytes and oligodendrocytes in the spinal cord white matter (data not shown). At the onset of disease, all four PLA₂s are expressed in infiltrating immune cells as shown above (Fig. 2A), which are located mainly in the submeningeal spaces (arrows in Fig. 3A–D). At the peak stage, iPLA₂ GVIA labelling is expressed mainly in infiltrating immune cells (Fig. 3F), while cPLA₂ GIVA, and sPLA₂ GIIA and GV, also show increased expression in astrocytes (Fig. 3E, G and H), and some oligodendrocytes (data not shown). There is also a more diffuse immunoreactivity for the two sPLA₂s in regions of EAE lesions at the peak stage of EAE (Fig. 3G and H), suggestive of staining of secreted protein. In the remission stage there is little if any labelling of cPLA₂ GIVA and iPLA₂ GVIA (Fig. 3I and J) but the expression of sPLA₂ GIIA and GV is still observed and remains high in astrocytes (Fig. 3K and L).

cPLA₂ GIVA and iPLA₂ GVIA play a role in the initiation of EAE

We assessed the role of these PLA₂s in initiating disease using two classes of small molecule inhibitors. cPLA₂ GIVA was blocked using

a 2-oxoamide compound (AX059) that is a highly selective and potent inhibitor of cPLA₂ GIVA (Table 1) (Kokotos *et al.*, 2004). This class of inhibitors has been extensively characterized (Kokotos *et al.*, 2004; Stephens *et al.*, 2006; Six *et al.*, 2007). iPLA₂ GVIA was blocked using a novel selective and potent fluoroketone compound (FKGK11) (Table 1) (Baskakis *et al.*, 2008; Lopez-Vales *et al.*, 2008). Two other novel pan-inhibitors that block all three types of PLA₂s (cPLA₂, iPLA₂ and sPLA₂) were also used: a fluoroketone (FKGK2) that blocks all three highly (86–92%), and a 2-oxoamide (AX115), which blocks all weakly (~50% range) (Table 1). Inhibitors were administered daily for 3 weeks starting 5 days after the immunization, i.e. before the onset of clinical symptoms (~Day 12). Mice were evaluated daily for clinical disability using a five-point scale (see Materials and methods section). Mice treated with the cPLA₂ GIVA inhibitor AX059, showed a significant reduction in the severity of the early course of the disease (Fig. 4), with abrogation of the first attack (clinical score of 0.5 at Day 18), but progressing into a second attack at Day 27. The end-point disability score at Day 40 was also lower than that of control EAE mice (Fig. 4). In sharp contrast, mice treated with the iPLA₂ inhibitor FKGK11 showed a marked reduction in clinical disability and progression of disease (Fig. 4). These mice reached a maximum peak clinical disability score of only grade 1.0 throughout the course of disease until Day 40, even though treatment was stopped at Day 25 (Fig. 4).

Mice treated with FKGK2, the strong pan-PLA₂ inhibitor showed a maximal score of ~0.5 for much of the 40 days, and was similar statistically with the results with FKGK11 (Fig. 4) suggesting that

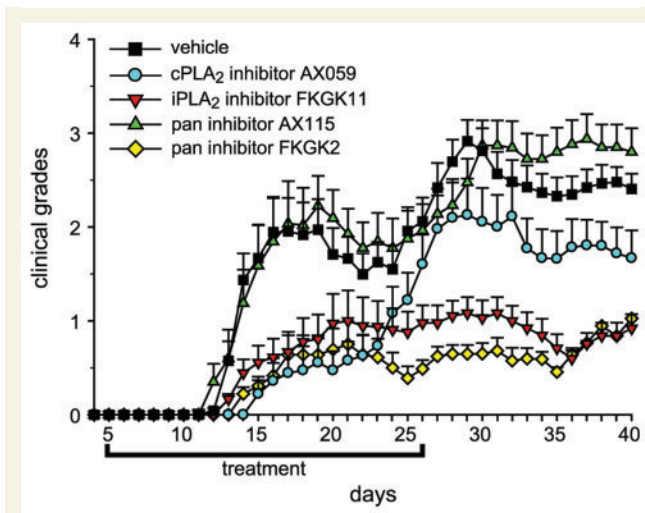


Figure 4 Effects of PLA₂ inhibitor treatment started before the onset of symptoms. Graph shows the clinical course of EAE in SJL/J mice that were treated with the cPLA₂ inhibitor (AX059), iPLA₂ inhibitor (FKGK11), a weak pan-PLA₂ inhibitor (AX115), and a strong pan-PLA₂ inhibitor (FKGK2). These inhibitors were administered before the onset of symptoms starting from Day 5 to Day 26; the EAE controls received vehicle injections. Data represent means \pm SEM of pooled data from two batches of mice; $n = 19$ mice in each group. The difference between the cPLA₂ inhibitor group and control group is significant during the first paralytic episode (Days 13–23; $P < 0.01$), suggesting that cPLA₂ has a role in initiation of disease. There is a marked reduction in severity of disease in mice treated with the iPLA₂ inhibitor, as compared to the control group throughout the course of disease (Days 14–40; $P < 0.01$), i.e. even after the treatment was stopped at Day 26. There is no statistically significant difference between the AX115 inhibitor treatment and vehicle-treated controls. The strong pan-PLA₂ inhibitor-treated (FKGK2) group showed a marked reduction in severity of disease as compared with the vehicle-treated control group throughout the course of disease (Days 14–40; $P < 0.01$), likely reflecting its ability to block cPLA₂ and iPLA₂.

the effect of the pan-inhibitor FKGK2 may be due to its ability to block iPLA₂. In contrast, the other pan-inhibitor (AX115) that blocks cPLA₂, iPLA₂ and sPLA₂ less effectively than FKGK2 did not differ from vehicle-treated controls (Fig. 4). Given the early start of the treatment, it is possible that the iPLA₂ inhibitor and pan-PLA₂ inhibitor (FKGK2) might affect the induction of EAE. Overall, these data suggest that cPLA₂ may play a role in the onset of EAE and iPLA₂ in the onset or induction of EAE.

iPLA₂ also plays a role in the progression and severity of EAE

To further assess the roles of cPLA₂ and iPLA₂ in the progression of EAE, inhibitor treatments were started after the onset of clinical symptoms, i.e. grade 0.5 (partial flaccid tail), which occurred starting at Day 11 or 12 (Fig 5). Treatment was continued for 2 weeks. Animals treated with the cPLA₂ inhibitor (AX059) showed slightly

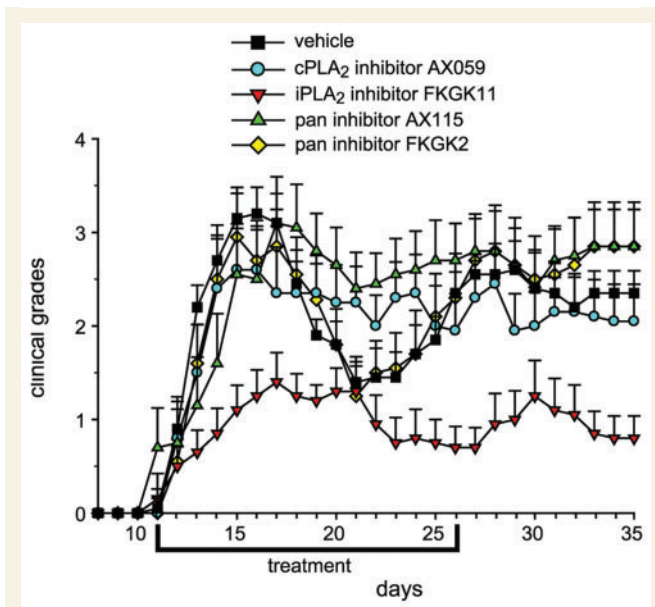


Figure 5 Effects of PLA₂ inhibitor treatment started after the onset of symptoms. Graph shows the clinical course of EAE in SJL/J mice that were treated with the cPLA₂ inhibitor (AX059), iPLA₂ inhibitor (FKGK11), the weak pan-PLA₂ inhibitor (AX115) and the strong pan-PLA₂ inhibitor (FKGK2), starting after the onset of clinical symptoms in the EAE animals. Data represent means \pm SEM of pooled data from two batches of mice; $n = 10$ mice in each group. Treatment with the cPLA₂ and iPLA₂ inhibitors was started after the mice started to show symptoms (clinical grade of 0.5, partial flaccid tail; starting on Days 11 and 12) and given for a 2-week period (indicated by the bar). Treatment with AX115 was started on Day 14 just before the mice reached the first clinical peak and given for a 2-week period. There is no statistically significant difference in the clinical scores between the cPLA₂ inhibitor treated and vehicle-treated control groups throughout the course of disease, suggesting that cPLA₂ may not play a role in the progression of disease. In contrast, the iPLA₂ inhibitor treated group shows a marked reduction in motor disability, suggesting that iPLA₂ plays a role in the progression of the disease (Days 13–35; $P < 0.01$). This effect persists after the treatment is stopped at Day 26. On the other hand, treatment with AX115 during the peak and remission stages resulted in a marked increase in the severity of the disease as compared to the vehicle-treated control group (Days 19–24; $P < 0.05$). The other pan-PLA₂ inhibitor-treated (FKGK2) group and the vehicle-treated control groups had scores that were not significantly different.

reduced scores but these differences are not statistically significant from the controls (Fig. 5), suggesting that although the cPLA₂ plays a role in the onset of the disease (Fig. 4), it may not be important in the progression phase. In contrast, mice treated after disease onset with the iPLA₂ inhibitor (FKGK11), showed marked improvement in clinical disability (Fig. 5), with a score of only 1.4 on Day 17, the peak of the first attack when the vehicle-treated mice have a score of 3.2. The beneficial effect persisted even after the termination of the treatment (Fig. 5). These data suggest that iPLA₂ may play role in the progression of the disease.

Treatment with the weak pan-PLA₂ inhibitor (AX115) worsened the disease, i.e. prevented the remission phase (Fig. 5). On Day 17, mice treated with AX115 had a mean peak score of grade 3, similar to the vehicle-treated group (Fig. 5). The vehicle-treated mice progressed into remission with an average score of ~1.4 at Day 23, while the AX115-treated mice had a worse clinical score of 2.5 (Fig. 5). By Day 35, the AX115-treated mice and vehicle treated EAE controls had a clinical score of 2.8 and 2.3, respectively. This effect is unlikely to be due to blocking of T cell apoptosis based on FACS analysis of annexin V labelling (data not shown). In striking contrast, the stronger pan-PLA₂ inhibitor-treated (FKGK2) group did not show any improvement (Fig. 5). The reasons for why the weaker pan-inhibitor has a worsening effect while the strong pan-inhibitor does not affect disease course is not known. However, the free acid product of the hydrolysis of AX115 inhibits sPLA₂ GIIA (IC₅₀=4.2 μm; M. Gelb and G. Kokotos, unpublished results). Therefore, the direct effects of AX115 and the conversion of AX115 to its free acid form *in vivo* could lead to greater inhibition of sPLA₂ while only partially blocking cPLA₂ and iPLA₂ as compared to FKGK2. Further studies are therefore warranted using more selective sPLA₂ inhibitors.

iPLA₂ inhibitor treatment reduces lesion burden

Histological analysis of lesion burden and myelin loss in the spinal cord was assessed at the end-point (Day 35) in mice treated after

the onset of symptoms. Only treatment with the iPLA₂ inhibitor (FKGK11), which was the only one to show clinical improvement when given after disease onset, had a statistically significant reduction in the number and size of EAE lesions in the spinal cord (Fig. 6A and C), as well as a reduction in the number of infiltrating immune cells per lesion (Fig. 6B).

Myelin loss was almost completely prevented in animals treated with either the cPLA₂ (AX059) or iPLA₂ (FKGK11) selective inhibitors (Fig. 6D–F). The strong pan-PLA₂ inhibitor-treated (FKGK2) animals also showed a significant reduction in myelin loss (Fig. 6D). In contrast, although the AX115-treated group showed a larger mean value, it was not significantly different from vehicle-treated controls (Fig. 6D). As mentioned above, this may be due to the somewhat greater selectivity of AX115 for sPLA₂ as compared with AX059 and FKGK11, and its ability to block cPLA₂ and iPLA₂ less effectively than FKGK2.

Effects of PLA₂ inhibitors on chemokine and cytokine expression

We assessed changes in the expression of 40 chemokines and cytokines, their receptors and related molecules at the protein level, using a mouse antibody array (RayBiotech Inc.). The analysis was carried out on spinal cords from mice treated with inhibitors starting from Day 5 post-immunization. Tissue was taken on Day 18 when the control vehicle-treated mice reached the peak of the first clinical attack. Twelve chemokines were increased in

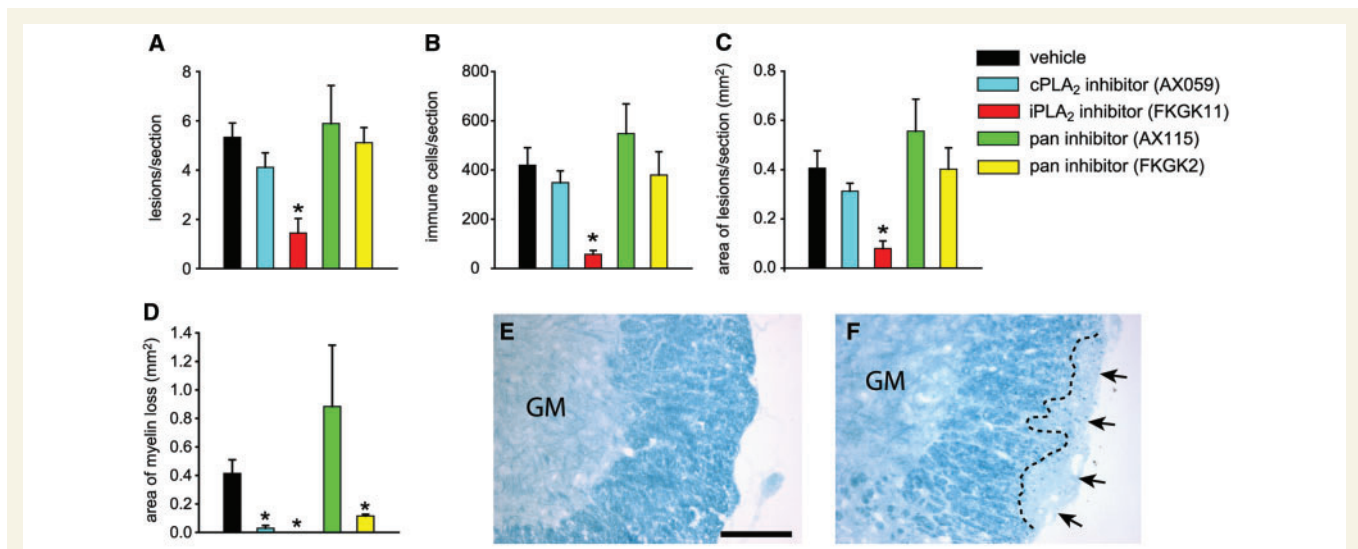


Figure 6 iPLA₂ inhibitor treatment reduces lesion burden and myelin loss. Quantitative analysis of lesion burden from H&E stained sections of the lumbar spinal cord from the end stage of EAE (Day 35) from delayed inhibitor treatments. The mice used for this analysis had similar clinical scores as the mean score for each group. Only the iPLA₂ inhibitor-treated (FKGK11) mice showed a significant reduction in (A) the number of lesions per cross section of the spinal cord, (B) the number of immune cells per cross section of the spinal cord, and (C) the area of the lesions (**P*<0.05). (D) Shows quantitative data of the size of areas showing myelin loss obtained from tissue sections stained with Luxol fast blue. Note that myelin loss is markedly reduced in both the cPLA₂ (AX059), iPLA₂ and the strong pan-PLA₂ inhibitor-treated (FKGK2) mice. AX115-treated mice show an increase in myelin loss although the variance between animals is very high. Luxol fast blue stained spinal cord sections from iPLA₂- (E) and vehicle-treated mice (F) are also shown. The areas showing myelin loss is outlined in the hatched lines in panel F. Data represent means ± SEM from three mice; three spinal cord sections were assessed per mouse (*n*=3 animals in each of the group). Scale bar = 100 μm.

vehicle-treated mice (Fig. 7), most of which are known to play a role in EAE, except for CXCL5 and CCL25, whose functions in CNS autoimmune disease remain unclear. The cPLA₂ GIVA (AX059) and iPLA₂ GVIA (FKGK11) selective inhibitors reduced 10 of the 12 chemokines that increase in vehicle-treated mice (Fig. 7), indicating that they prevent the robust inflammatory cascade seen in EAE. In contrast, the weak pan-inhibitor AX115, which inhibits sPLA₂ more than AX059 or FKGK11, differed from the latter two, reducing the expression of seven of the 12 chemokines (Fig. 7). Importantly, it increased the expression of CCL5 (9.6-fold), CCL9 (9.7-fold) and CCL24 (1.8-fold), (Fig. 7), which can also regulate the allergic arm of the immune response. The strong pan-PLA₂ inhibitor (FKGK2) reduced the expression of 10 of the 12 chemokines (Fig. 7) but also increased the expression of CCL5 (3.6-fold) and CCL9 (3-fold), but to a lesser extent than AX115. The marked upregulation of CCL5, CCL9 and CCL24 by AX115 as compared to FKGK2 indicates that it does not act like a weaker version of FKGK2. Whether the AX115 effect is due to its effects on sPLA₂ will need to be investigated further.

Similar profiling of cytokine protein expression revealed that 13 cytokines and related molecules were increased in vehicle-treated EAE mice (Fig. 8), all of which have been shown to play a role in EAE. The cPLA₂ and iPLA₂ selective inhibitors both reduced expression of 11 of the 13 pro-inflammatory cytokines (Fig. 8), as well as increased the expression of the anti-inflammatory cytokine IL-10 (~1.5-fold; Fig. 8). AX115 on the other hand reduced expression of nine of the 13 cytokines, but importantly, it failed to

increase IL-10 (Fig. 8), and caused a marked increase in soluble TNF receptor 1 (sTNFR1) (~4-fold) (Fig. 8). The lack of increase in IL-10 after treatment with the AX115 is worth noting because this cytokine plays an important role in the remission stage of EAE (Samoilova *et al.*, 1998). Also, blocking with sTNFR exacerbates disease in multiple sclerosis patients (van Oosten *et al.*, 1996; Kollias and Kontoyiannis, 2002). The other pan-PLA₂ inhibitor (FKGK2) also reduced the expression of nine of the 13 pro-inflammatory cytokines (Fig. 8) but showed a pattern that has characteristics of the cPLA₂ and iPLA₂ inhibitors on the one hand and AX115 on the other, i.e. it showed increased expression of IL-10 (2-fold), as well as that of the sTNFR1 (3.4-fold) (Fig. 8).

PLA₂ inhibitors induce differential inhibition and hydrolysis of fatty acids

As PLA₂s hydrolyze fatty acids from the *sn*-2 position of phospholipids, we carried out a comprehensive profiling of 40 fatty acids that are attached to five phospholipid classes in extracts of spinal cords. These tissues were taken from the same groups of mice used for the chemokine/cytokine assay described above.

Changes in vehicle-treated EAE mice

Vehicle-treated EAE mice showed increased hydrolysis and release of 11 fatty acids from the phosphatidylcholine, cardiolipin and phosphatidylethanolamine classes for a total of 18 fatty acid/phospholipid combinations, as compared with naïve animals (Fig. 9;

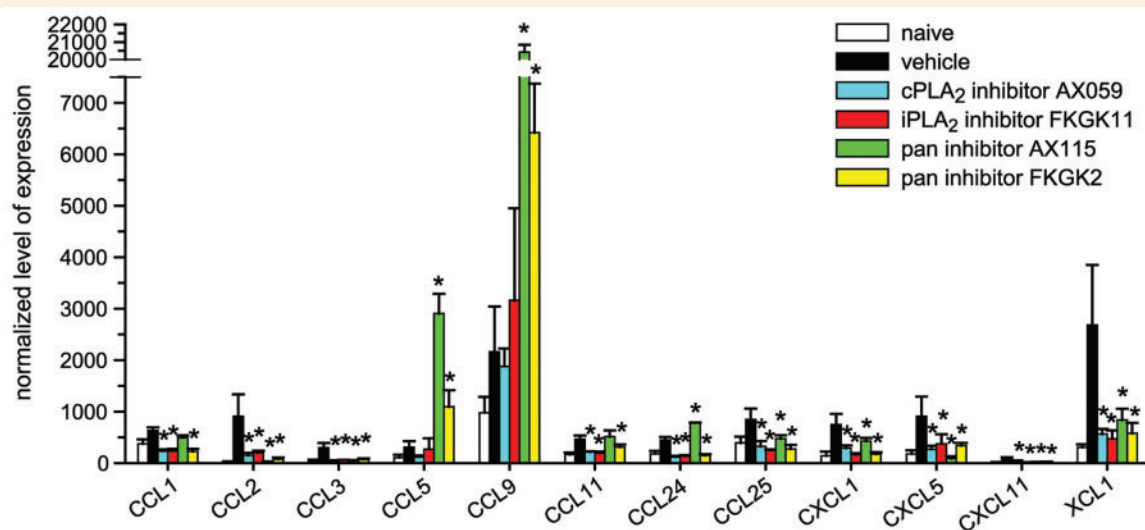


Figure 7 Changes in chemokine protein expression in PLA₂ inhibitor treated mice. Graph shows the level chemokine expression at the protein level in spinal cords of naïve mice and EAE mice treated with various PLA₂ inhibitors starting on Day 5. Tissues were taken on Day 18, when the vehicle-treated animals reached the peak of the first clinical attack. The cPLA₂ and iPLA₂ inhibitor treatments resulted in a significant reduction in 10 chemokines (**P* < 0.01). AX115 inhibitor treatment reduced the expression of seven chemokines (**P* < 0.01), but also greatly increased the expression of CCL24, CCL5 and CCL9 (**P* < 0.01). The strong pan-PLA₂ inhibitor (FKGK2) reduced the expression of 10 chemokines (**P* < 0.01) and also increased the expression of CCL5 and CCL9 (**P* < 0.01), but to a lesser extent than AX115. Data represent mean ± SEM. Experiments were repeated 3 times with samples from different mice; (*n* = 3). Asterisk represents a statistically significant difference (*P* < 0.01) as compared to vehicle-treated EAE controls. [CCL1 (TCA-3), CCL2 (MCP-1), CCL3 (MIP-1 α), CCL5 (RANTES), CCL9 (MIP-1 γ), CCL11 (Eotaxin), CCL24 (Eotaxin-2), CCL25 (TECK), CXCL1 (KC), CXCL5 (LIX), CXCL11 (I-TAC), XCL1 (Lymphotactin)].

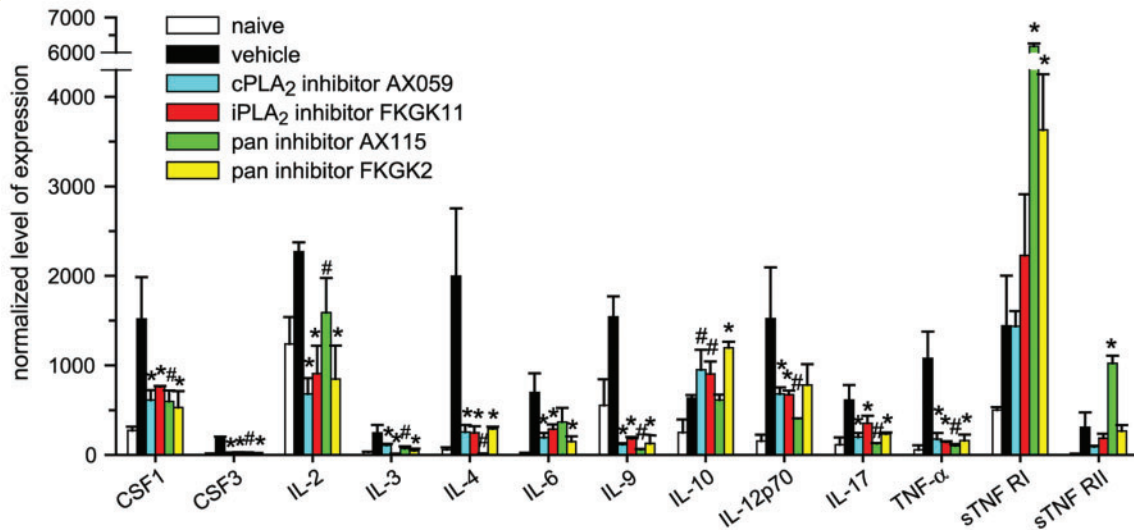


Figure 8 Changes in cytokine protein expression in PLA₂ inhibitor treated mice. Graph shows the level chemokine expression at the protein level in spinal cords of naïve mice and EAE mice treated with various PLA₂ inhibitors starting on Day 5. Tissues were taken on Day 18, when the vehicle-treated animals reached the peak of the first clinical attack. The cPLA₂ and iPLA₂ inhibitor treatments resulted in a significant reduction in 10 cytokines ($*P < 0.01$), as well as increased the expression of the anti-inflammatory cytokine IL-10 ($\#P < 0.05$). AX115 reduced the expression of 9 cytokines ($\#P < 0.05$) while having no effect on IL-10. It also caused a significant increase in soluble TNF receptors 1 and 2 ($*P < 0.01$). The pan- PLA₂ inhibitor (FKGK2) also reduced the expression of 9 cytokines ($*P < 0.01$) and increased expression of IL-10 ($*P < 0.01$), as well as that of the soluble TNF receptor 1 ($*P < 0.01$). Data represent mean \pm SEM. Experiments were repeated three times with samples from different mice; ($n = 3$) $\#P < 0.05$ and $*P < 0.01$ represents statistically significant differences as compared with vehicle-treated EAE controls. [CSF1 (MCSF), CSF3 (GMCSF)].

Table 2). Four of these (stearic, palmitic, arachidic and behenic acids) are saturated fatty acids, which have pro-inflammatory functions (Kontogianni *et al.*, 2006). Nervonic acid, which shows 22 and 28% release from phosphatidylethanolamine and phosphatidylcholine, respectively, plays a role in myelin biosynthesis (Sargent *et al.*, 1994) and is decreased in postmortem brain tissue from multiple sclerosis patients (Gerstl *et al.*, 1972; Sargent *et al.*, 1994). Moreover, the release of nine fatty acids from phosphatidylcholine would lead to the generation of lysophosphatidylcholine, a potent demyelinating agent that can also induce chemokine/cytokine expression in the CNS (Ousman and David, 2001). Additionally, in vehicle-treated EAE mice there is a 67% release of eicosapentaenoic acid (EPA) (Fig. 9; Table 2), which leads to the production of the series-3 prostaglandins and series-5 leukotrienes (Calder, 2002), and the E-series of resolvins (Ariel and Serhan, 2007). These fatty acid metabolites have anti-inflammatory properties and could put the brakes on the inflammation at the peak stage of EAE and thus lead to the onset of remission seen in these animals.

Changes in lipid profiles in pan-PLA₂ inhibitor treated mice

The strong pan-PLA₂ inhibitor FKGK2 prevented the hydrolysis of 14 of the 18 fatty acid/phospholipid combinations released from vehicle-treated EAE mice, and reduced the hydrolysis of four fatty acids (Fig. 9; Table 2). It increased the release of tetracosahexanoic acid (23%) from phosphatidylserine. This fatty acid is a precursor to docosahexaenoic acid (DHA), which

has anti-inflammatory properties, and has been shown to give rise to the D-series of resolvins (Ariel and Serhan, 2007) and decrease cytokines such as IL-6, IL-1 β and TNF- α (Das, 2006; Simopoulos, 2006). However, FKGK2 only partially blocked the release of four fatty acids from phosphatidylcholine (Fig. 9 and Table 2), suggesting that treatment with this inhibitor would still give rise to lysophosphatidylcholine, which may account for the continued inflammation in these mice (Fig. 6A–C). In contrast AX115 also prevented the hydrolysis of 13 of the 18 fatty acid/phospholipid combinations hydrolyzed in the vehicle-treated EAE mice (Fig. 9; Table 2). Six fatty acids (arachidic, eicosapentaenoic (EPA), eicosenoic, erucic, tetracosahexanoic and 1-enyl-octadecenoic acids) were still significantly hydrolyzed in the AX115-treated mice (Fig. 9; Table 2). On the other hand, three fatty acids, continued to be released from phosphatidylcholine, which could lead to the generation of lysophosphatidylcholine that can trigger inflammation and demyelination.

Changes in lipid profiles in cPLA₂ and iPLA₂ inhibitor treated mice

The cPLA₂ inhibitor (AX059) prevented the hydrolysis of all fatty acids from phospholipids that were increased in EAE and yields a similar lipid composition profile as naïve animals (Fig. 9). Only the cPLA₂ inhibitor was able to prevent the production of PGE₂, thromboxane B₂ (TXB₂), 11-HETE and 15-HETE that are pro-inflammatory (Supplementary Fig. 2). This is consistent with cPLA₂ being the main regulator of arachidonic acid release that gives rise to these eicosanoids (Kudo and Murakami, 2002).

Table 2 Mean \pm SD of the fatty acid hydrolysis

	Naïve (nmol)	Treatment (nmol)	Difference (%)	P-value
Vehicle-treated EAE versus naïve				
Cardiolipin–palmitic	3122.3 \pm 371.7	2272.8 \pm 111.9	27.2	0.03
Cardiolipin–arachidic	464.0 \pm 69.4	278.8 \pm 64.6	39.9	0.02
Cardiolipin–eicosapentaenoic	16.1 \pm 4.8	5.3 \pm 4.8	67.1	0.05
Cardiolipin–docosadienoic	34.1 \pm 5.3	21.2 \pm 5.1	37.3	0.03
Phosphatidylcholine–stearic	5723.5 \pm 164.5	5349.8 \pm 61.4	6.5	0.03
Phosphatidylcholine–behenic	115.8 \pm 8.1	94.8 \pm 3.1	18.2	0.02
Phosphatidylcholine–vaccenic	3978.5 \pm 165.3	3423.4 \pm 102.4	14.0	0.01
Phosphatidylcholine–arachidic	347.9 \pm 20.1	249.9 \pm 16.6	28.2	0.001
Phosphatidylcholine–oleic	13980.0 \pm 393.1	1196.5 \pm 550.6	14.4	0.001
Phosphatidylcholine–eicosenoic	1666.2 \pm 46.4	1227.6 \pm 47.3	26.3	0.001
Phosphatidylcholine–erucic	177.1 \pm 7.8	127.7 \pm 7.4	27.9	0.001
Phosphatidylcholine–nervonic	47.7 \pm 4.2	37.5 \pm 2.7	21.4	0.02
Phosphatidylcholine–docosadienoic	90.4 \pm 10.7	66.9 \pm 3.8	26.0	0.03
Phosphatidylethanolamine–arachidic	589.3 \pm 43.4	464.8 \pm 7.8	21.1	0.01
Phosphatidylethanolamine–vaccenic	2043.2 \pm 138.8	1694.6 \pm 111.7	17.1	0.03
Phosphatidylethanolamine–erucic	341.4 \pm 16.2	267.7 \pm 14.7	21.6	0.001
Phosphatidylethanolamine–eicosapentaenoic	45.2 \pm 8.6	27.3 \pm 5.2	39.6	0.05
Phosphatidylethanolamine–docosadienoic	25.7 \pm 4.4	15.4 \pm 1.0	39.9	0.03
cPLA ₂ inhibitor (AX059)-treated EAE versus naïve				
No increase in release of fatty acids. Fatty acid hydrolysis restored to naïve levels				
iPLA ₂ inhibitor (FKGK11)-treated EAE versus naïve				
Cardiolipin–arachidic	464.0 \pm 69.4	273.7 \pm 60.4	41.0	0.02
Cardiolipin–eicosapentaenoic	16.1 \pm 4.8	5.5 \pm 4.8	65.8	0.05
Cardiolipin–eicosadienoic	146.2 \pm 22.6	98.3 \pm 2.4	32.8	0.04
Cardiolipin–docosadienoic	34.1 \pm 5.3	19.6 \pm 1.4	42.6	0.01
Cardiolipin–docosapentaenoic	17.2 \pm 2.0	5.3 \pm 4.6	69.1	0.02
lysoPhosphatidylcholine–eicosapentaenoic	1.0 \pm 0.2	0.2 \pm 0.3	80.0	0.03
pan-PLA ₂ inhibitor (FKGK2)-treated EAE versus naïve				
Phosphatidylcholine–arachidic	347.9 \pm 20.1	289.4 \pm 29.1	16.8	0.05
Phosphatidylcholine–vaccenic	3978.5 \pm 165.3	3535.7 \pm 135.7	11.1	0.02
Phosphatidylcholine–oleic	13980.0 \pm 393.1	12569.1 \pm 630.5	10.1	0.03
Phosphatidylcholine–eicosenoic	1666.2 \pm 46.4	1377.6 \pm 101.4	17.3	0.01
Phosphatidylserine–tetracosahexanoic	9.7 \pm 0.8	7.5 \pm 0.3	22.8	0.01
pan inhibitor (AX115)-treated EAE versus naïve				
Cardiolipin–arachidic	464.0 \pm 69.4	324.4 \pm 27.5	30.1	0.04
Cardiolipin–eicosapentaenoic	16.1 \pm 4.8	3.2 \pm 5.5	80.3	0.03
Phosphatidylcholine–arachidic	347.9 \pm 20.1	269.4 \pm 24.9	22.5	0.01
Phosphatidylcholine–eicosenoic	1666.2 \pm 46.4	1393.4 \pm 52.5	16.4	0.001
Phosphatidylcholine–erucic	177.1 \pm 7.8	177.1 \pm 7.8	22.4	0.001
Phosphatidylserine–tetracosahexanoic	9.7 \pm 0.8	6.4 \pm 0.6	33.8	0.001
Phosphatidylserine–1-enyl-octadecenoic	217.4 \pm 37.9	133.3 \pm 32.5	38.7	0.04

Data given in Fig. 9, $n=3$ in each group. $P<0.05$ (Student's t -test).

CNS (Fig. 10A–C). In addition, iPLA₂⁺ immune cells were also present in regions with active lesions as indicated by the presence of large numbers of macrophages (Fig. 10D–F). Some of these iPLA₂ cells are macrophages (arrows in Fig. 10F).

Discussion

Our previous work using AACOCF₃, a non-selective inhibitor which blocks all intracellular cytosolic PLA₂s, including cPLA₂

GIVA and iPLA₂ GVIA, showed that they play an important role in the onset and progression of EAE in the C57BL/6 mouse strain that has a naturally occurring null mutation of sPLA₂ GIIA (Kennedy *et al.*, 1995). Furthermore, cPLA₂ GIVA null mice are not susceptible to EAE induction (Marusic *et al.*, 2005). Our current findings, using the cPLA₂ selective inhibitor (AX059) now indicate that that cPLA₂ GIVA may play a role only in the onset of EAE. We also show that iPLA₂ GVIA on the other hand may play a role in the onset as well as the progression of EAE. When given before the onset of symptoms, both inhibitors have a

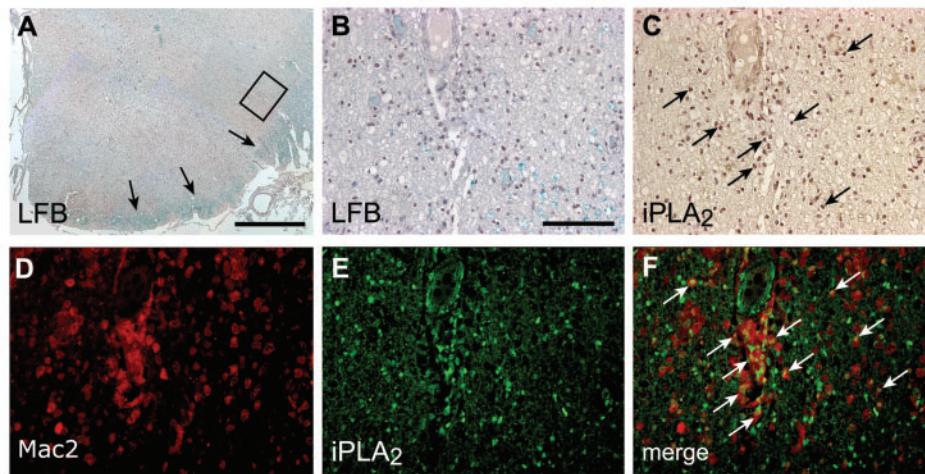


Figure 10 Expression of iPLA₂ in human multiple sclerosis. (A) Ventral funiculus of the spinal cord from a patient with secondary progressive multiple sclerosis stained with Luxol fast blue to visualize myelin which is seen mainly along the periphery of the section (arrows) and counterstained with haematoxylin. Note the loss of myelin in the ventral funiculus. (B and C) Shows higher magnification of the area outlined in panel A. Tissue section stained with Luxol fast blue and haematoxylin (B) and iPLA₂ (C). Note the presence of iPLA₂ positive cells (arrows in C) in the area of the demyelinated lesion. (D–F) Double-immunofluorescence labelling for Mac-2 (activated macrophages) (D), and iPLA₂ (E) from an active lesion. (F) Note in the merged image the presence of activated macrophages expressing iPLA₂ (arrows). Scale bars: A = 3 mm, B–F = 100 μ m.

profound effect in reducing the expression of 75% of the chemokines and pro-inflammatory cytokines that are upregulated in EAE, while also increasing the expression of the beneficial cytokine IL-10. These inhibitors also reduced the hydrolysis of fatty acids from phospholipids that are involved in pro-inflammatory processes. The saturated fatty acid family has collectively been shown to contribute to pro-inflammatory responses (Karsten *et al.*, 1994; Ajuwon and Spurlock, 2005; Kontogianni *et al.*, 2006; Stentz and Kitabchi, 2006), e.g. stearic and palmitic acid are able to induce the expression of IL-1 β , IL-2, IFN- γ and TNF- α (Karsten *et al.*, 1994), which are cytokines involved in the pathogenesis of multiple sclerosis and EAE. As expected, only the cPLA₂ GIVA inhibitor was able to reduce eicosanoid production from arachidonic acid. Since iPLA₂ GVIA inhibitor treatment had a profound effect in reducing the severity of the disease, it suggests that inhibiting the arachidonic acid pathway alone is not sufficient to curtail disease progression after the appearance of symptoms. Although eicosanoid production is seen in EAE and in patients with multiple sclerosis (Dore-Duffy *et al.*, 1991; Whitney *et al.*, 2001), treatment with COX and lipoxygenase inhibitors, or a combination of both, showed varying results (Weber and Hempel, 1989; Simmons *et al.*, 1992). This suggests the need to also regulate other metabolites of PLA₂ action, such as generation of lysophosphatidylcholine that can impact on both inflammation and demyelination.

The fluoroketone inhibitor that selectively blocks iPLA₂ reduces the severity of the disease even when treatment was started after the onset of symptoms, and this protective effect persisted after the treatment was terminated. The main difference between the cPLA₂ and iPLA₂ inhibitor treatment that we detected was the release of 65% of the omega-3, EPA, from cardiolipin and 80% from lysophosphatidylcholine by iPLA₂ inhibitor treatment.

EPA is known for its anti-inflammatory effects and studies implementing dietary interventions in multiple sclerosis patients, particularly with omega-3 fatty acids, appear to show improvements in disease outcome (Bates *et al.*, 1989; Nordvik *et al.*, 2000; Weinstock-Guttman *et al.*, 2005). EPA can also be converted by cellular cytochrome P450 monooxygenase and 5-lipoxygenase to generate the E-series of resolvins, which are potent anti-inflammatory mediators (Arita *et al.*, 2005; Serhan, 2007). Moreover, the release of 80% of the fatty acid EPA from lysophosphatidylcholine in the iPLA₂ inhibitor treated group is likely to neutralize its demyelinating and pro-inflammatory properties. In addition, the iPLA₂ inhibitor prevented the hydrolysis of all fatty acids from phosphatidylcholine that occurs in vehicle-treated EAE mice, thus reducing the production of lysophosphatidylcholine. In contrast, AX115 and the pan-inhibitor FKGK2 still allowed the hydrolysis of a number of fatty acids from phosphatidylcholine. The absence of lysophosphatidylcholine production may contribute importantly to the reduction in chemokines and pro-inflammatory cytokines seen after iPLA₂ inhibitor treatment. Treatment with the iPLA₂ inhibitor also results in the release of 69% of the docosapentaenoic acid from cardiolipin, a precursor of DHA. The latter can generate natural lipoxins, protectins and resolvins of the D series (Ariel and Serhan, 2007; Serhan, 2007) that actively terminate inflammation. The iPLA₂ inhibitor reduced the expression of 10 out of 12 chemokines and all 10 pro-inflammatory cytokines that are increased in EAE. Interestingly, it increased the expression of IL-10, an anti-inflammatory cytokine. The iPLA₂ selective inhibitor could therefore mediate its effects via multiple mechanisms: preventing the hydrolysis of pro-inflammatory fatty acids and permitting the release of protective ones; reducing the production of lysophosphatidylcholine; reducing pro-inflammatory chemokine/cytokine expression and increasing expression anti-inflammatory ones; and

neutralizing lysophosphatidylcholine, a potent demyelinating and pro-inflammatory agent. These experiments therefore suggest that selective blocking of iPLA₂ GVIA may be effective in treating CNS autoimmune disease such as multiple sclerosis, especially since iPLA₂ is expressed in immune cells in multiple sclerosis lesions.

We found that the expression of sPLA₂ is increased in the remission phase of EAE. There are two earlier reports that blocking sPLA₂ is protective in EAE when started prior to the onset of symptoms (Pinto *et al.*, 2003; Cunningham *et al.*, 2006). The inhibitors used in these two earlier studies, however, appear to have other activities, such as neuronal survival and antioxidant properties. On the other hand, our data indicate that AX115 worsens disease severity when given after the onset of EAE. Based on its inhibitory profile, AX115 appears as a weaker pan-PLA₂ inhibitor than FKGG2. However, its biological effects on chemokine and cytokine expression and disease progression are not compatible with it being a weaker form of FKGG2. In fact the effects of these two pan-inhibitors are quite divergent. As mentioned above, the free acid derivative of the hydrolysis of AX115 was found to be a potent inhibitor of sPLA₂ GIIA; this combined with the ability of AX115 to partially block sPLA₂ directly, could suggest that *in vivo*, AX115 might inhibit sPLA₂ significantly as compared to AX059 and FKGG11, while only partially blocking the other PLA₂s. However, whether these effects are due to inhibition of sPLA₂ needs to be investigated further with more selective inhibitors. There is evidence in the literature that sPLA₂ may play a role in the resolution of inflammation in an acute model of pleurisy (Gilroy *et al.*, 2004). Treatment with AX115 also increases the expression of CCL24, CCL5 and CCL9 in EAE. CCL24 is selectively chemotactic for eosinophils (Rothenberg and Hogan, 2006); CCL5 induces chemotaxis of T cells and monocytes, and also activates eosinophils (Rothenberg and Hogan, 2006); and CCL9, induces chemotaxis of T cells and activates neutrophils (Poltorak *et al.*, 1995), suggesting activation of the allergic arm of the EAE response to exacerbate disease and prevent remission. Treatment with AX115 failed to upregulate the Th-2 cytokine IL-10, which may also underlie the worsening of the disease. It also increased by 4-fold the expression of the sTNFR1 which has been shown to exacerbate disease in multiple sclerosis patients (van Oosten *et al.*, 1996; Kollias and Kontoyiannis, 2002). Further work is warranted to establish if these effects are due to inhibition of sPLA₂ or due to partial blocking of all three PLA₂s during the peak and remission phase of EAE.

The results presented here show that cPLA₂ GIVA may play a role in the onset of EAE, while iPLA₂ GVIA may contribute importantly to the onset and progression of the disease. It also suggests that the beneficial effects of iPLA₂ inhibition may be mediated via a number of mechanisms such as regulating chemokine and cytokine expression, and the types of fatty acids hydrolyzed from membrane phospholipids. iPLA₂ GVIA may therefore be an excellent therapeutic target for the treatment of the CNS autoimmune disease multiple sclerosis.

Supplementary material

Supplementary material is available at *Brain* online.

Acknowledgements

The authors also thank Margaret Attiwell for preparing the illustrations.

Funding

Canadian Institutes of Health Research; MS Society of Canada (to S.D.); Greek Ministry of Education (EPEAEK program, European Union 75%—Greek government 25%) (to G.K.); US National Institutes of Health (GM 20508 to E.A.D.); CIHR Studentship (to A.K.). Canadian Institutes of Health Research postdoctoral fellowship (to R.L.V.).

References

- Ajuwon KM, Spurlock ME. Palmitate activates the NF-kappaB transcription factor and induces IL-6 and TNFalpha expression in 3T3-L1 adipocytes. *J Nutr* 2005; 135: 1841–6.
- Ariel A, Serhan CN. Resolvins and protectins in the termination program of acute inflammation. *Trends Immunol* 2007; 28: 176–83.
- Arita M, Clish CB, Serhan CN. The contributions of aspirin and microbial oxygenase to the biosynthesis of anti-inflammatory resolvins: novel oxygenase products from omega-3 polyunsaturated fatty acids. *Biochem Biophys Res Commun* 2005; 338: 149–57.
- Baskakis C, Magrioti V, Cotton N, Stephens D, Constantinou-Kokotou V, Dennis EA, et al. Synthesis of polyfluoro ketones for selective inhibition of human phospholipase A(2) Enzymes. *J Med Chem* 2008; 51: 8027–37.
- Bates D, Carlidge NE, French JM, Jackson MJ, Nightingale S, Shaw DA, et al. A double-blind controlled trial of long chain n-3 polyunsaturated fatty acids in the treatment of multiple sclerosis. *J Neurol Neurosurg Psychiatry* 1989; 52: 18–22.
- Baxter AG. The origin and application of experimental autoimmune encephalomyelitis. *Nat Rev Immunol* 2007; 7: 904–12.
- Calder PC. Dietary modification of inflammation with lipids. *Proc Nutr Soc* 2002; 61: 345–58.
- Calder PC. N-3 polyunsaturated fatty acids and inflammation: from molecular biology to the clinic. *Lipids* 2003; 38: 343–52.
- Compston A, Coles A. Multiple sclerosis. [erratum appears in *Lancet* 2002; 360: 648]. *Lancet* 2002; 359: 1221–31.
- Cunningham TJ, Yao L, Oettinger M, Cort L, Blankenhorn EP, Greenstein JJ. Secreted phospholipase A2 activity in experimental autoimmune encephalomyelitis and multiple sclerosis. *J Neuroinflammation* 2006; 3: 26.
- Das UN. Essential fatty acids: biochemistry, physiology and pathology. *Biotechnol J* 2006; 1: 420–39.
- Dore-Duffy P, Ho SY, Donovan C. Cerebrospinal fluid eicosanoid levels: endogenous PGD2 and LTC4 synthesis by antigen-presenting cells that migrate to the central nervous system. *Neurology* 1991; 41: 322–4.
- Folch J, Lees M, Sloane Stanley GH. A simple method for the isolation and purification of total lipides from animal tissues. *J Biol Chem* 1957; 226: 497–509.
- Gerstl B, Tavaststjerna MG, Eng LF, Smith JK. Sphingolipids and their precursors in human brain (normal and MS). *Z Neurol* 1972; 202: 104–20.
- Gilroy DW, Newson J, Sawmynaden P, Willoughby DA, Croxtall JD. A novel role for phospholipase A2 isoforms in the checkpoint control of acute inflammation. *FASEB J* 2004; 18: 489–98.
- Gold R, Linington C, Lassmann H. Understanding pathogenesis and therapy of multiple sclerosis via animal models: 70 years of merits and culprits in experimental autoimmune encephalomyelitis research. *Brain* 2006; 129: 1953–71.

- Huang J, Aki T, Yokochi T, Nakahara T, Honda D, Kawamoto S, et al. Grouping newly isolated docosahexaenoic acid-producing thraustochytrids based on their polyunsaturated fatty acid profiles and comparative analysis of 18S rRNA genes. *Mar Biotechnol (NY)* 2003; 5: 450–7.
- Kalyvas A, David S. Cytosolic phospholipase A2 plays a key role in the pathogenesis of multiple sclerosis-like disease. *Neuron* 2004; 41: 323–35.
- Karsten S, Schafer G, Schauder P. Cytokine production and DNA synthesis by human peripheral lymphocytes in response to palmitic, stearic, oleic, and linoleic acid. *J Cell Physiol* 1994; 161: 15–22.
- Kennedy BP, Payette P, Mudgett J, Vadas P, Pruzanski W, Kwan M, et al. A natural disruption of the secretory group II phospholipase A2 gene in inbred mouse strains. *J Biol Chem* 1995; 270: 22378–85.
- Kokotos CG, Baskakis C, Kokotos G. Synthesis of medicinally interesting polyfluoro ketones via perfluoroalkyl lithium reagents. *J Org Chem* 2008; 73: 8623–6.
- Kokotos G, Kotsovolou S, Six DA, Constantinou-Kokotou V, Beltzner CC, Dennis EA. Novel 2-oxoamide inhibitors of human group IVA phospholipase A(2). *J Med Chem* 2002; 45: 2891–3.
- Kokotos G, Six DA, Loukas V, Smith T, Constantinou-Kokotou V, Hadjipavlou-Litina D, et al. Inhibition of group IVA cytosolic phospholipase A2 by novel 2-oxoamides in vitro, in cells, and in vivo. *J Med Chem* 2004; 47: 3615–28.
- Kollias G, Kontoyiannis D. Role of TNF/TNFR in autoimmunity: specific TNF receptor blockade may be advantageous to anti-TNF treatments. *Cytokine Growth Factor Rev* 2002; 13: 315–21.
- Kontogianni MD, Zampelas A, Tsigos C. Nutrition and inflammatory load. *Ann NY Acad Sci* 2006; 1083: 214–38.
- Kudo I, Murakami M. Phospholipase A2 enzymes. *Prostaglandins Other Lipid Mediat* 2002; 68–69: 3–58.
- Lopez-Vales R, Navarro X, Shimizu T, Baskakis C, Kokotos G, Constantinou-Kokotou V, et al. Intracellular phospholipase A2 group IVA and group VIA play important roles in Wallerian degeneration and axon regeneration after peripheral nerve injury. *Brain* 2008; 131: 2620–31.
- Marusic S, Leach MW, Pelker JW, Azoitei ML, Uozumi N, Cui J, et al. Cytosolic phospholipase A2 alpha-deficient mice are resistant to experimental autoimmune encephalomyelitis. *J Exp Med* 2005; 202: 841–51.
- Nordvik I, Myhr KM, Nyland H, Bjerve KS. Effect of dietary advice and n-3 supplementation in newly diagnosed MS patients. *Acta Neurol Scand* 2000; 102: 143–9.
- Noseworthy JH, Lucchinetti C, Rodriguez M, Weinshenker BG. Multiple sclerosis. [see comment]. *N Engl J Med* 2000; 343: 938–52.
- Ousman SS, David S. Lysophosphatidylcholine induces rapid recruitment and activation of macrophages in the adult mouse spinal cord. *Glia* 2000; 30: 92–104.
- Ousman SS, David S. MIP-1alpha, MCP-1, GM-CSF, and TNF-alpha control the immune cell response that mediates rapid phagocytosis of myelin from the adult mouse spinal cord. *J Neurosci* 2001; 21: 4649–56.
- Pinto F, Brenner T, Dan P, Krinsky M, Yedgar S. Extracellular phospholipase A2 inhibitors suppress central nervous system inflammation. *Glia* 2003; 44: 275–82.
- Poltorak AN, Bazzoni F, Smirnova, II, Alejos E, Thompson P, Luheshi G, et al. MIP-1 gamma: molecular cloning, expression, and biological activities of a novel CC chemokine that is constitutively secreted in vivo. *J Inflamm* 1995; 45: 207–19.
- Rocha PN, Plumb TJ, Coffman TM. Eicosanoids: lipid mediators of inflammation in transplantation. *Springer Semin Immunopathol* 2003; 25: 215–27.
- Rothenberg ME, Hogan SP. The eosinophil. *Annu Rev Immunol* 2006; 24: 147–74.
- Samoilova EB, Horton JL, Chen Y. Acceleration of experimental autoimmune encephalomyelitis in interleukin-10-deficient mice: roles of interleukin-10 in disease progression and recovery. *Cell Immunol* 1998; 188: 118–24.
- Sargent JR, Coupland K, Wilson R. Nervonic acid and demyelinating disease. *Med Hypotheses* 1994; 42: 237–42.
- Schaloske RH, Dennis EA. The phospholipase A2 superfamily and its group numbering system. *Biochim Biophys Acta* 2006; 1761: 1246–59.
- Serhan CN. Resolution phase of inflammation: novel endogenous anti-inflammatory and proresolving lipid mediators and pathways. *Annu Rev Immunol* 2007; 25: 101–37.
- Simmons RD, Hugh AR, Willenborg DO, Cowden WB. Suppression of active but not passive autoimmune encephalomyelitis by dual cyclooxygenase and 5-lipoxygenase inhibition. *Acta Neurol Scand* 1992; 85: 197–9.
- Simopoulos AP. Evolutionary aspects of diet, the omega-6/omega-3 ratio and genetic variation: nutritional implications for chronic diseases. *Biomed Pharmacother* 2006; 60: 502–7.
- Six DA, Barbayianni E, Loukas V, Constantinou-Kokotou V, Hadjipavlou-Litina D, Stephens D, et al. Structure-activity relationship of 2-oxoamide inhibition of group IVA cytosolic phospholipase A2 and group V secreted phospholipase A2. *J Med Chem* 2007; 50: 4222–35.
- Steinman L, Martin R, Bernard C, Conlon P, Oksenberg JR. Multiple sclerosis: deeper understanding of its pathogenesis reveals new targets for therapy. *Ann Rev Neurosci* 2002; 25: 491–505.
- Steinman L, Zamvil SS. How to successfully apply animal studies in experimental allergic encephalomyelitis to research on multiple sclerosis. *Ann Neurol* 2006; 60: 12–21.
- Stentz FB, Kitabchi AE. Palmitic acid-induced activation of human T-lymphocytes and aortic endothelial cells with production of insulin receptors, reactive oxygen species, cytokines, and lipid peroxidation. *Biochem Biophys Res Commun* 2006; 346: 721–6.
- Stephens D, Barbayianni E, Constantinou-Kokotou V, Peristeraki A, Six DA, Cooper J, et al. Differential inhibition of group IVA and group VIA phospholipases A2 by 2-oxoamides. *J Med Chem* 2006; 49: 2821–8.
- Trapp BD, Peterson J, Ransohoff RM, Rudick R, Mork S, Bo L. Axonal transection in the lesions of multiple sclerosis. *N Engl J Med* 1998; 338: 278–85.
- van der Valk P, De Groot CJ. Staging of multiple sclerosis (MS) lesions: pathology of the time frame of MS. *Neuropathol Appl Neurobiol* 2000; 26: 2–10.
- van Oosten BW, Barkhof F, Truyen L, Boringa JB, Bertelmann FW, von Blomberg BM, et al. Increased MRI activity and immune activation in two multiple sclerosis patients treated with the monoclonal anti-tumor necrosis factor antibody cA2. *Neurology* 1996; 47: 1531–4.
- Weber F, Hempel K. Protection against experimental allergic encephalomyelitis with complete Freund's adjuvant is unaffected by prostaglandin synthesis inhibition. *Int Arch Allergy Appl Immunol* 1989; 89: 242–5.
- Weinstock-Guttman B, Baier M, Park Y, Feichter J, Lee-Kwen P, Gallagher E, et al. Low fat dietary intervention with omega-3 fatty acid supplementation in multiple sclerosis patients. *Prostaglandins Leukot Essent Fatty Acids* 2005; 73: 397–404.
- Whitney LW, Ludwin SK, McFarland HF, Biddison WE. Microarray analysis of gene expression in multiple sclerosis and EAE identifies 5-lipoxygenase as a component of inflammatory lesions. *J Neuroimmunol* 2001; 121: 40–8.
- Yaksh TL, Kokotos G, Svensson CI, Stephens D, Kokotos CG, Fitzsimmons B, et al. Systemic and intrathecal effects of a novel series of phospholipase A2 inhibitors on hyperalgesia and spinal prostaglandin E2 release. *J Pharmacol Exp Ther* 2006; 316: 466–75.